Computers in Biology and Medicine 135 (2021) 104627

Contents lists available at ScienceDirect

Computers in Biology and Medicine

journal homepage: www.elsevier.com/locate/compbiomed

Preload & Frank-Starling curves, from textbook to bedside: Clinically applicable non-additionally invasive model-based estimation in pigs

Rachel Smith [a,*], J. Geoffrey Chase [a], Christopher G. Pretty [a], Shaun Davidson [b], Geoffrey M. Shaw [c], Thomas Desaive [d]

[a] Department of Mechanical Engineering, University of Canterbury, New Zealand
[b] Institute of Biomedical Engineering, University of Oxford, United Kingdom
[c] Christchurch Hospital Intensive Care Unit, New Zealand
[d] IGA Cardiovascular Science, University of Liège, Liège, Belgium

ARTICLE INFO

Keywords:
Preload
Frank-starling curves
Hemodynamic monitoring
Intensive care unit
Fluid responsiveness
End-diastolic volume

ABSTRACT

Background: Determining physiological mechanisms leading to circulatory failure can be challenging, contributing to the difficulties in delivering effective hemodynamic management in critical care. Continuous, non-additionally invasive monitoring of preload changes, and assessment of contractility from Frank-Starling curves could potentially make it much easier to diagnose and manage circulatory failure.

Method: This study combines non-additionally invasive model-based methods to estimate left ventricle end-diastolic volume (*LEDV*) and stroke volume (*SV*) during hemodynamic interventions in a pig trial (N = 6). Agreement of model-based *LEDV* and measured admittance catheter *LEDV* is assessed. Model-based *LEDV* and *SV* are used to identify response to hemodynamic interventions and create Frank-Starling curves, from which Frank-Starling contractility (*FSC*) is identified as the gradient.

Results: Model-based *LEDV* had good agreement with measured admittance catheter *LEDV*, with Bland-Altman median bias [limits of agreement (2.5th, 97.5th percentile)] of 2.2 ml [-13.8, 22.5]. Model *LEDV* and *SV* were used to identify non-responsive interventions with a good area under the receiver-operating characteristic (ROC) curve of 0.83. *FSC* was identified using model *LEDV* and *SV* with Bland-Altman median bias [limits of agreement (2.5th, 97.5th percentile)] of 0.07 [-0.68, 0.56], with *FSC* from admittance catheter *LEDV* and aortic flow probe *SV* used as a reference method.

Conclusions: This study provides proof-of-concept preload changes and Frank-Starling curves could be non-additionally invasively estimated for critically ill patients, which could potentially enable much clearer insight into cardiovascular function than is currently possible at the patient bedside.

1. Introduction

Hemodynamic monitoring is important for diagnosing and managing circulatory failure, a leading cause of ICU mortality [1,2]. However, hemodynamic monitoring is hindered by inability to accurately, continuously, and/or non-invasively measure key variables relating to cardiac and vascular function [3]. Thus, it can be challenging for clinicians to elucidate physiological mechanisms contributing to circulatory failure, which is of key importance for effective hemodynamic management [4].

Preload, the strain of the left ventricle prior to contraction, is central to understanding cardiovascular physiology and a vital clinical consideration for fluid resuscitation [5]. Increases in preload lead to increased stroke volume (*SV*) due to the Frank-Starling mechanism where increased strain in cardiac muscle prior to contraction causes increased force of contraction [6]. *In vivo*, left ventricle end-diastolic volume (*LEDV*) is an accepted surrogate measure of preload [5,7].

Frank-Starling curves show the relationship between preload and *SV*. The slope of this curve, Frank-Starling contractility (*FSC*), is a new construct defined as the extent to which changes in ventricular filling induce a change in *SV*. *FSC* = 0.5 means for every 1 ml increase in *LEDV*, *SV* increases by 0.5 ml. Thus, *FSC* reflects the force-length relation of cardiac muscle which is a function of cardiac muscle contractility, and afterload. It is important to clarify, *FSC* is distinct from fluid-

* Corresponding author.
E-mail address: rachel.smith@pg.canterbury.ac.nz (R. Smith).

https://doi.org/10.1016/j.compbiomed.2021.104627
Received 9 May 2021; Received in revised form 13 June 2021; Accepted 29 June 2021
Available online 3 July 2021

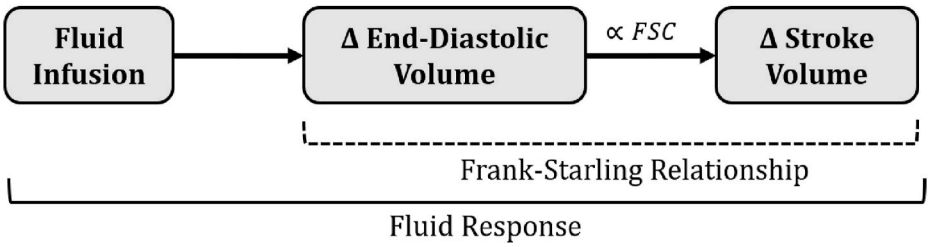

Fig. 1. *SV* response to a fluid infusion depends upon both the *LEDV* response to fluids and the subsequent *SV* response to *LEDV*, which is governed by the Frank-Starling relationship.

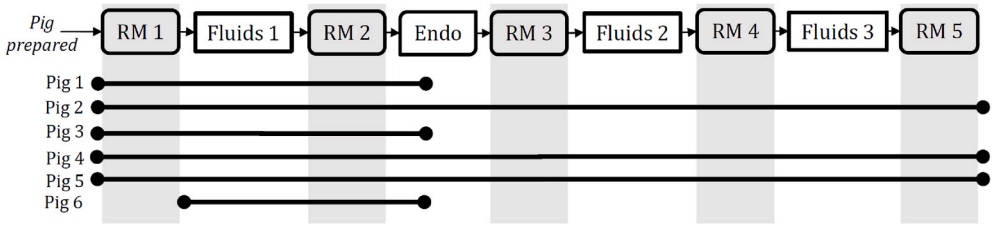

Fig. 2. Time-schedule of experimental interventions, and data used for each pig. Interventions are respiratory recruitment manoeuvres (RM), fluid infusions (Fluids) and endotoxin infusion (Endo).

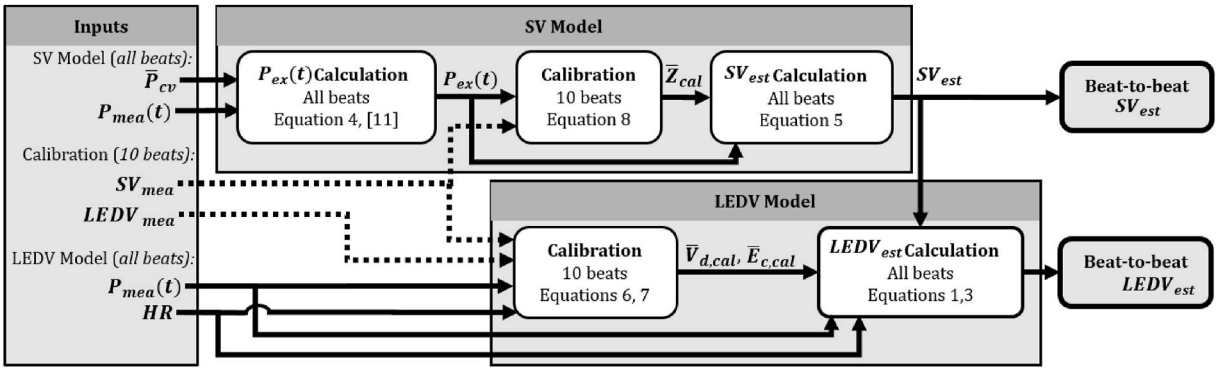

Fig. 3. Overview of *SV* & *LEDV* estimation method, reading left to right. Model inputs are typically available ICU measures: arterial pressure waveform (P_{mea}), beat-wise average central venous pressure ($\overline{P}_{cv}$), and *HR*. A short period of calibration SV_{mea} and $LEDV_{mea}$ are also required. Models provide beat-to-beat calibrated estimates of *SV* & *LEDV*.

responsiveness. *FSC* characterises the Frank-Starling relationship, whereas fluid-responsiveness, defined as how well a patient's *SV* responds to fluid resuscitation, encompasses both the fluid-*LEDV* relationship and the Frank-Starling relationship, as illustrated in Fig. 1. Assessment of *FSC* and *LEDV* could potentially allow monitoring of the extent to which preload and *SV* are altered by treatment or changing patient condition, enabling monitoring of contractility changes as *FSC* and quantification of fluid responsiveness, a "holy-grail" goal of critical care practice [8,9].

This study combines non-additionally invasive methods to estimate *LEDV* [10] and *SV* [11] to create Frank-Starling curves during hemodynamic interventions in a porcine animal trial. Model-based *LEDV* is validated using directly measured *LEDV* from an admittance catheter. Similarly, *FSC* from model-estimated Frank-Starling curves is validated using directly measured Frank-Starling curves. In a clinical setting, these direct measurements are not feasible. Therefore, the non-additionally invasive model-estimated *LEDV* and Frank-Starling curves presented could potentially enable much clearer insight into cardiovascular function than is currently possible at the patient bedside.

2. Materials and methods

2.1. Porcine trials and measurements

Pig experiments were conducted at the Centre Hospitalier Universitaire de Liège, Belgium and approved by the Ethics Committee of the University of Liège Medical Faculty, permit number 14–1726.

N = 6 pure Piétrain pigs were used, weighing 18.5 kg–29.0 kg. Diazepam (1 mg kg^{-1}) and Zoletil (0.1 mL kg^{-1}) were used for initial sedation and anesthesia. A continuous infusion of sufentanil (0.1 mL kg^{-1} h^{-1} at 0.005 mg mL^{-1}), Thiobarbital (0.1 mL kg^{-1} h^{-1}) and Nimbex (1 mL kg^{-1} h^{-1} at 2 mg mL^{-1}) were used to maintain sedation and anesthesia, delivered via superior vena cava catheter. Pigs were mechanically ventilated via tracheostomy with baseline positive end-expiratory pressure (PEEP) of 5 cmH_2O and tidal volume of 10 mL kg^{-1} delivered by a GE Engstrom CareStation mechanical ventilator (GE 92 Healthcare, Waukesha, WI, USA).

Blood pressure was measured in the proximal aorta (P_{ao}), femoral artery (P_{fem}), and vena cava (P_{cv}) using high fidelity pressure catheters (Transonic, Ithaca, NY, USA). Left ventricle pressures and volumes (V_{LV}) were measured using 7F micromanometer-tipped admittance catheters (Transonic Scisense Inc., Ontario, Canada). Aortic flow (Q_{ao}) was

Table 1
Identification of non-responsive interventions using d_{95}. * indicates non-responsive interventions ($d_{95,mea} < 0.200$, $d_{95,est} < 0.276$). *T/F* shows whether $d_{95,est}$ successfully predicts a non-responsive intervention (TN: True Negative, TP: True Positive, FN: False Negative, FP: False Positive).

Intervention		$d_{95,mea}$	$d_{95,est}$	T/F
Pig 1	RM 1	0.59	0.54	TN
	Fluids 1	0.25	0.11*	FP
	RM 2	0.63	0.74	TN
	Endo	0.53	0.80	TN
Pig 2	RM 1	0.43	0.36	TN
	Fluids 1	0.08*	0.07*	TP
	RM 2	0.37	0.26*	FP
	Endo	0.40	0.26*	FP
	RM 3	0.57	0.37	TN
	Fluids 2	0.14*	0.17*	TP
	RM 4	0.45	0.33	TN
	Fluids 3	0.13*	0.10*	TP
	RM 5	0.54	0.39	TN
Pig 3	RM 1	0.41	0.67	TN
	Fluids 1	0.19*	0.23*	TP
	RM 2	0.33	0.48	TN
	Endo	0.67	0.92	TN
Pig 4	RM 1	0.27	0.32	TN
	Fluids 1	0.18*	0.27*	TP
	RM 2	0.30	0.31	TN
	Endo	0.27	0.25*	FP
	RM 3	0.34	0.54	TN
	Fluids 2	0.13*	0.40	FN
	RM 4	0.68	0.55	TN
	Fluids 3	0.35	0.39	TN
	RM 5	0.58	0.55	TN
Pig 5	RM 1	0.21	0.27*	FP
	Fluids 1	0.21	0.17*	FP
	RM 2	0.15*	0.18*	TP
	Endo	0.27	0.19*	FP
	RM 3	0.26	0.24*	FP
	Fluids 2	0.16*	0.27*	TP
	RM 4	0.31	0.28	TN
	Fluids 3	0.19*	0.24*	TP
	RM 5	0.32	0.63	TN
Pig 6	Fluids 1	0.20	0.12*	FP
	RM 2	0.51	0.32	TN
	Endo	0.46	0.39	TN

measured from an ultrasonic aortic flow probe positioned around the proximal aorta near the aortic valve (Transonic, Ithaca, NY, USA). Once the probe was located, the thorax was held closed using clamps.

All data was recorded at a sampling rate of 250 Hz as a single Notocord data file (Instem, Croissy-sur-Seine, France). Signals were filtered with a 5th order Butterworth low-pass filter, with a cut-off frequency of 20 Hz (P_{fem}, P_{ao}, P_{cv}) and 10 Hz for noisier signals (V_{LV}, Q_{ao}).

Pigs underwent several types of intervention: respiratory recruitment manouevres (RM) in which PEEP is increased in steps of 5 cmH_2O to PEEP of $\geq$15 cmH_2O to reduce systemic venous return and thus *SV* [12]; fluid infusions of 500 mL of saline solution over 30 min to increase circulatory volume and ventricular preload; and an infusion of endotoxin (E. Coli lipopolysaccharide at 0.5 mg kg^{-1} over 30 min) to produce a septic shock like response [13].

Fig. 2 shows the order of interventions and data used for each pig. Pig 6 RM 1 was not used due to faulty V_{LV} readings during the RM. Pigs 1, 3, and 6 died during the endotoxin infusion. The model was calibrated during 10 beats of stable hemodynamics for each intervention, and, subsequently, the ability of model-based estimates to track changes in response to each intervention was assessed.

2.2. Measurement of LEDV and SV for validation

Measured *SV* (SV_{mea}) is used for validation and calibration as measured from integrating an ultrasonic aortic flow probe signal (Q_{ao}) over one beat for Pigs 2–6. Beats are separated using the foot (t_0) of Q_{ao}, identified using a shear-transform algorithm [14]. Flow probes are quoted as having precision of ±2% [15]. For Pig 1, admittance catheter V_{LV} is used to obtain *SV* as the range of V_{LV} over one beat, due to non-physiological flow probe Q_{ao} for this pig. Measured *LEDV* ($LEDV_{mea}$) was calculated from an admittance catheter as the maximum V_{LV} of each beat. Admittance catheter *LEDV* has Bland-Altman mean bias [limits of agreement (1.96 standard deviation)] of −5.6 ml [-18.5, 7.3] using real-time 3D echocardiography as a reference method [16].

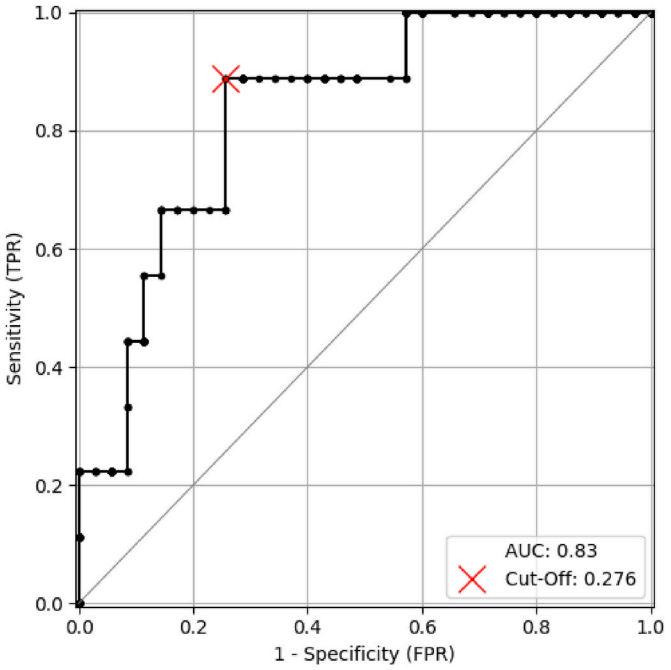

Fig. 4. ROC curve for non-responsive intervention identification using $d_{95,est}$, with $d_{95,mea}$ as a reference method. The chosen cut-off $d_{c,est}$ of 0.276 maximises $TPR - FPR$.

2.3. Non-additionally invasive LEDV estimation

LEDV is estimated from an input arterial pressure waveform signal (P_{mea}) and heart rate (*HR*) using a method from Ref. [10]. P_{fem} is used for input P_{mea}, except Pig 4 where P_{ao} is used due to faulty P_{fem} measurements. *LEDV* is estimated as the sum of *SV* and V_{es}:

$$LEDV_{est} = V_{es,est} + SV_{est} \tag{1}$$

V_{es}, the left ventricle end-systolic volume, is estimated using the end-systolic pressure-volume relation [17]:

$$P_{es} = E_{es} \times (V_{es} - V_0) \tag{2}$$

where P_{es} is ventricle end-systolic pressure, V_0 is ventricle volume at zero pressure, and E_{es} is end-systolic elastance, a parameter depending upon contractility and loading conditions [18]. To make these terms clinically identifiable, the following assumptions are made:

- P_{es} can be estimated as $P_{es,mea}$, the P_{mea} pressure at the end of systole. End-systolic time, t_{es}, is identified using a weighted second derivative algorithm presented elsewhere [19]. This approach assumes the arterial catheter site for P_{mea} is sufficiently near the heart that resistance is small, and thus there is negligible pressure drop.
- V_0 can be replaced with V_d, ventricle deadspace, a reasonable assumption as V_0 and V_d are often used interchangeably and have similar physiological values [17]. V_d is estimated to be 0.48 V_{es} [10].
- E_{es} is modelled as $E_c \times HR^3$. *HR* is used as an indicator of E_{es} changes, and E_c is a constant, identified through calibration, representing subject-specific coupling between *HR* and E_{es} [10]. This relationship

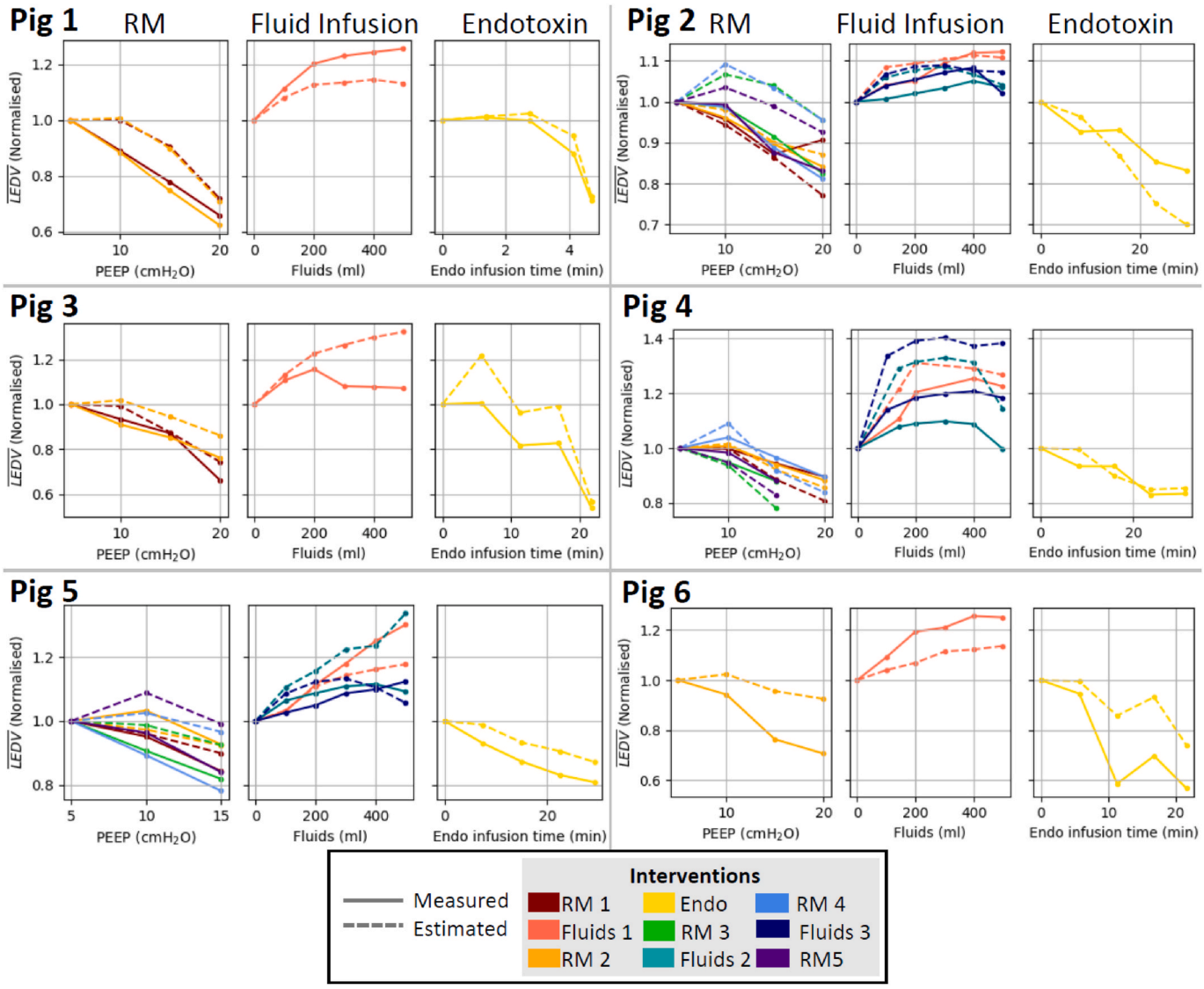

Fig. 5. $\overline{LEDV}$ changes in response to each intervention type (recruitment manoeuvre, fluid infusion, endotoxin infusion) for each pig. $\overline{LEDV}$ is normalised using the first step of each intervention, thus has no units.

is used because *HR* changes are typically mathematically sympathetic with changes in E_{es}, as regulatory mechanisms, such as the neural regulatory baroreflex, act on both, rather than each independently [20]. *HR* is calculated using the foot-to-foot time of P_{mea}, and filtered with a median filter (kernel size = 11) to mitigate the impact of abnormal beats which do not correspond to E_{es} changes.

Using these surrogate terms and rearranging for $V_{es,est}$, Equation (2) becomes [10]:

$$V_{es,est} = \frac{P_{es,mea}}{E_c \times HR^3} + V_d \tag{3}$$

2.4. Non-additionally invasive SV estimation

SV is estimated from the 3-element Windkessel model implementation in Ref. [11]. This pulse contour analysis model relates pressure and flow in the arteries using three lumped parameters (*Z*, *R*, *C*) representing resistance and compliance of the systemic circulation [21]. Model inputs are an arterial pressure waveform (P_{mea}), and pressure of the downstream venous system which is assumed constant over a given beat, equal to the average P_{cv} during that beat, $\overline{P}_{cv}$.

Input P_{mea} is divided into a reservoir component (P_{res}) associated with filling the large arteries and an excess component (P_{ex}), which is directly proportional to flow into the circulation (Q_{in}):

$$P_{mea}(t) = P_{res}(t) + P_{ex}(t) \tag{4}$$

P_{res} is calculated from P_{mea} as an optimisation problem for a given beat by enforcing the condition there is no flow into the aorta during diastole, as presented in Ref. [11]. Knowing P_{res}, Equation (4) can be used to calculate P_{ex}. Hence, *SV* for each beat is calculated from integrating Q_{in}, knowing $Q_{in} = \frac{P_{ex}}{Z}$:

$$SV_{est,\,n} = \frac{1}{Z}\int_{t_{0,n}}^{t_{0,n+1}} P_{ex}(\tau)\, d\tau \tag{5}$$

where the n^{th}beat begins and ends at P_{mea} waveform foot t_0, detected using a shear-transform algorithm [14], and *Z* is obtained from calibration.

2.5. Calibration

SV_{est} and $LEDV_{est}$ were calibrated during 10 beats of stable recording at the beginning of each intervention in Fig. 2 for each pig using SV_{mea}

Table 2
FSC and R^2 from the Frank-Starling curve line of best fit for each pig and intervention. NR indicates non-responsive interventions ($d_{95,mea} < 0.200$) for which no line of best fit was calculated. * indicates R^2 not meeting acceptable criterion ($R^2 < 0.65$). *FSC* error is calculated as $FSC_{est} - FSC_{mea}$. Note, *FSC* and R^2 have no units.

Intervention		*FSC*		*FSC* error	R^2	
		mea	est		mea	est
Pig 1	RM 1	0.46	0.50	0.04	0.91	0.94
	Fluids 1	0.54	0.23	−0.30	0.94	0.91
	RM 2	0.48	0.59	0.11	0.96	0.99
	Endo	0.35	0.53	0.18	0.93	1.00
Pig 2	RM 1	0.81	0.52	−0.29	0.71	0.94
	Fluids 1	NR	–	–	–	–
	RM 2	0.60	0.52	−0.08	0.87	0.91
	Endo	0.62	0.29	−0.33	0.65	0.97
	RM 3	0.29	0.53	0.24	0.73	0.86
	Fluids 2	NR	–	–	–	–
	RM 4	0.41	0.46	0.05	0.66	0.83
	Fluids 3	NR	–	–	–	–
	RM 5	0.52	0.53	0.01	0.94	0.83
Pig 3	RM 1	0.27	0.76	0.49	0.60*	0.99
	Fluids 1	NR	–	–	–	–
	RM 2	0.33	0.76	0.43	0.86	0.98
	Endo	0.40	0.60	0.20	0.96	0.99
Pig 4	RM 1	0.93	0.59	−0.34	0.85	0.97
	Fluids 1	NR	–	–	–	–
	RM 2	0.56	0.57	0.01	0.87	0.96
	Endo	0.51	0.40	−0.10	0.80	0.90
	RM 3	0.79	0.60	−0.19	0.81	0.99
	Fluids 2	NR	–	–	–	–
	RM 4	1.27	0.59	−0.68	0.88	0.92
	Fluids 3	0.86	0.50	−0.36	0.73	0.86
	RM 5	1.09	0.65	−0.44	0.94	0.66
Pig 5	RM 1	0.17	0.62	0.45	0.16*	0.95
	Fluids 1	0.20	0.38	0.18	0.66	0.97
	RM 2	NR	–	–	–	–
	Endo	0.43	0.50	0.07	0.89	0.95
	RM 3	0.19	0.56	0.37	0.49*	0.88
	Fluids 2	NR	–	–	–	–
	RM 4	0.11	0.67	0.56	0.16*	0.96
	Fluids 3	NR	–	–	–	–
	RM 5	0.28	0.59	0.32	0.48*	0.96
Pig 6	Fluids 1	0.16	0.29	0.13	0.71	0.91
	RM 2	0.21	0.50	0.29	0.83	0.88
	Endo	0.13	0.36	0.22	0.77	0.77

and $LEDV_{mea}$, with the exception of Pig 4 fluid interventions, and the first fluid intervention for Pigs 2 and 3. These interventions were calibrated at the end of the intervention as fluid administrations began during unstable hemodynamics with rapidly changing blood pressure following the RMs. Parameters identified from calibration ($\overline{V}_{d,cal}$, $\overline{E}_{c,cal}$, $\overline{Z}_{cal}$) were used for the remaining beats of each intervention. Clinically, calibration of SV_{mea} and $LEDV_{mea}$ could be obtained non-invasively using echocardiography.

$V_{d,cal,n}$ and $E_{c,cal,n}$ are identifed for the nth calibration beat by rearranging Equations (1) and (3), respectively:

$$V_{d,cal,n} = 0.48 \times V_{es,n} = 0.48(LEDV_{mea,n} - SV_{mea,n}) \tag{6}$$

$$E_{c,cal,n} = \frac{P_{es,mea,n}}{HR_n^3 \times \left(LEDV_{mea,n} - SV_{mea,n} - \overline{V}_{d,cal}\right)} \tag{7}$$

$Z_{cal,n}$ is found for each calibration beat using a rearrangement of Equation (5):

$$Z_{cal,\,n} = \frac{1}{SV_{mea,\,n}} \int_{t_{0,n}}^{t_{0,n+1}} P_{ex}(\tau)\, d\tau \tag{8}$$

Beat-wise calibration values ($V_{d,cal,n}$, $E_{c,cal,n}$, $Z_{cal,\,n}$) are averaged across the 10 calibration beats to reduce the impact of measurement noise, obtaining a single value for each parameter ($\overline{V}_{d,cal}$, $\overline{E}_{c,cal}$, $\overline{Z}_{cal}$).

The sequence of steps for model-based SV_{est} and $LEDV_{est}$ estimation is:

1. Inputs are measured/calculated: model input *HR*, P_{mea}, $\overline{P}_{cv}$ for all beats, and calibration SV_{mea} & $LEDV_{mea}$ for 10 beats
2. P_{ex} is calculated for all beats from inputs P_{mea}, $\overline{P}_{cv}$ using *SV* model (Equation (4) [11])
3. $\overline{Z}_{cal}$ is calculated to calibrate P_{ex} and thus *SV* model using SV_{mea} for 10 beats (Equation (8))
4. SV_{est} is calculated from $\overline{Z}_{cal}$, P_{ex} for all beats (Equation (5))
5. $\overline{V}_{d,cal}$, $\overline{E}_{c,cal}$ are calculated to calibrate *LEDV* model using inputs P_{mea}, *HR* and 10 beats of SV_{mea} & $LEDV_{mea}$ (Equations (6) and (7))
6. $LEDV_{est}$ is calculated for all beats using calibration parameters $\overline{V}_{d,cal}$, $\overline{E}_{c,cal}$ and inputs P_{mea}, *HR* (Equations(1) and (3))

The outcome is beat-to-beat $LEDV_{est}$ and SV_{est}. This process is shown in Fig. 3.

2.6. Analysis

2.6.1. Response to interventions

Non-responsive interventions were identified using the distance, *d*, of each [$LEDV_{mea}$, SV_{mea}] pair from the intervention mean [$LEDV_{mea}$, SV_{mea}] value. A 7-beat median filter of $LEDV_{mea}$ and SV_{mea} was calculated to mitigate the impact of abnormal heart beats, and measurement noise. For each intervention, *LEDV* & *SV* measurements were normalised by dividing them by their respective intervention mean. The Euclidean distance, *d*, of each normalised measurement from the mean was identified. The use of normalised measurements enables direct comparison between subjects.

An intervention was considered non-responsive if the 95th percentile of *d*, d_{95}, was less than the cut-off value $d_{c,mea} = 0.2$, which represents measurements with *LEDV/SV* changes less than 20% from the mean. In these cases, $LEDV_{mea}$ & SV_{mea} changes are small relative to $LEDV_{mea}$ measurement precision, where admittance catheter *LEDV* has Bland-Altman limits of agreement as large as 23% using real-time 3D echocardiography as a reference method [16]. Hence, within this limit, the *LEDV-SV* relationship cannot be reliably identified. This method for determining a response acknowledges either a change in *LEDV* or *SV* represents a change in hemodynamic state, and an intervention could successfully alter *LEDV* without altering *SV*, or vice versa. This analysis aims to identify non-responsive interventions, given the potential clinical harm of fluid overload from delivering fluids to non-responsive patients [9]. Hence, a non-response is considered "positive", and a response is considered "negative".

The ability of SV_{est} & $LEDV_{est}$ to successfully identify non-responsive interventions from $d_{95,est}$ is assessed using receiver-operator characteristic (ROC) analysis [22]. Specifically, $d_{95,est}$ is calculated for each pig and intervention in the same manner as d_{95}, but using model-based SV_{est} & $LEDV_{est}$. The non-responsive intervention cut-off threshold ($d_{c,est}$) was varied, producing a ROC curve of false positive rate (*FPR*) vs. true positive rate (*TPR*). The optimal cut-off value ($d_{c,est}$) was chosen to maximise both sensitivity (*TPR*) and specificity (1 − *FPR*). Area under the curve (AUC) and balanced accuracy are used to provide a measure of diagnostic accuracy of the model for identifying non-responsive interventions.

2.7. LEDV estimation

Average $LEDV_{mea}$ and $LEDV_{est}$ for each step of each intervention type, $\overline{LEDV}_{mea}$ and $\overline{LEDV}_{est}$, is calculated. For RMs, average *LEDV* at each PEEP level is identified. For fluid infusions, the final 50 beats are averaged from each 100 ml portion of the infusion. For endotoxin infusions and shock, 50 beats are averaged at 5 time points spread evenly across the

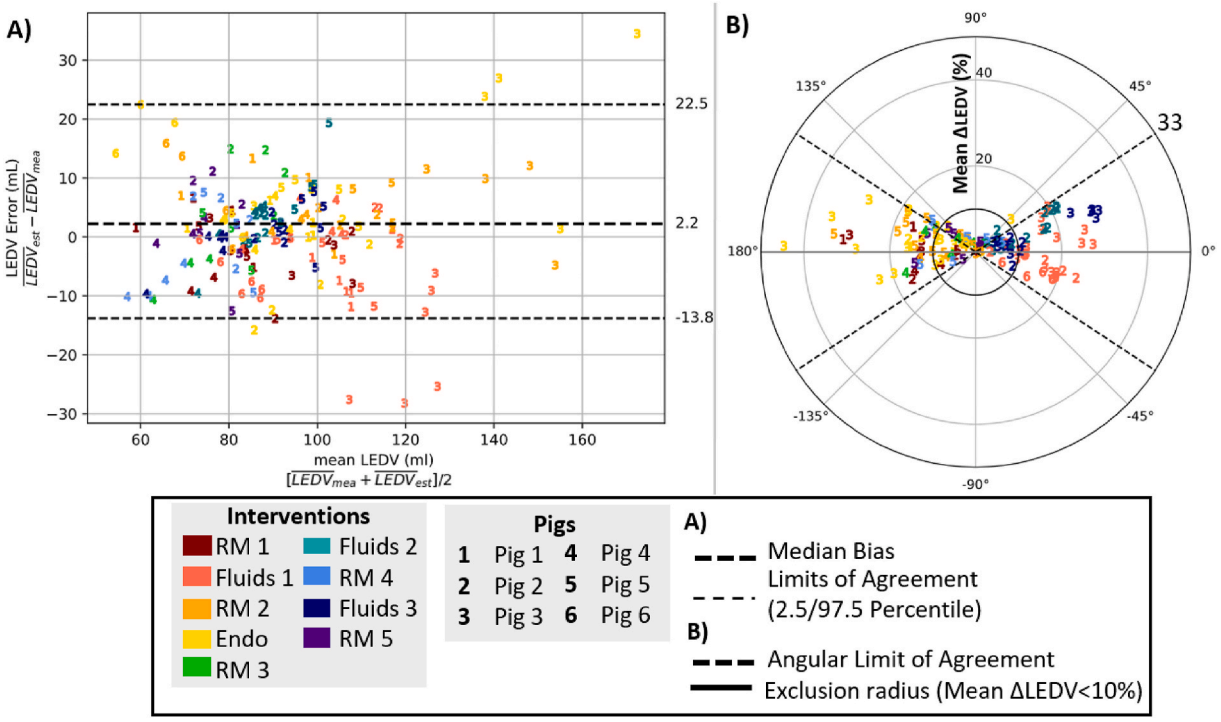

Fig. 6. A) Bland-Altman plot showing agreement of $\overline{LEDV}_{est}$ and $\overline{LEDV}_{mea}$. B) Polar plot shows trending ability of $\overline{LEDV}_{est}$ against $\overline{LEDV}_{mea}$.

duration of the 30 min infusion (Pigs 2,4,5), or from the beginning of the infusion until death (Pigs 1,3,6). Averaging of *LEDV* in this manner aims to reduce noise corresponding to *LEDV* changes not caused by the intervention.

The agreement between $\overline{LEDV}_{mea}$ and $\overline{LEDV}_{est}$ values is assessed by Bland-Altman analysis [23]. Median bias and 95% range [2.5th, 97.5th percentiles] are used for limits of agreement, ensuring no assumption is made about how error is distributed. Acceptable limits are ±35 ml based on reported 95% limits of agreement of [-59, 11 ml] from contrast echocardiography compared against MRI [24]. The defined acceptable limits allow for a similar range of measurements, but expect 0 bias for this calibrated method.

Model ability to capture *LEDV* trends is assessed by polar plot analysis [25] using $\overline{LEDV}_{mea}$ and $\overline{LEDV}_{est}$. For each *LEDV* measurement an X–Y pair of Δ*LEDV* percentage changes is calculated (X: $\Delta\overline{LEDV}_{mea}$, Y: $\Delta\overline{LEDV}_{est}$). Polar angle ($\theta$) is calculated as the angle of divergence of the Δ*LEDV* X–Y vector from the identity line Y = X. Radius is the mean percentage change of the two methods. Trending ability is assessed using angular limits of agreement, defined as the larger value of the 2.5th & 97.5th percentile of θ, calculated with angles converted to a [-90°, +90°] range. Only sufficiently large Δ*LEDV* are used in calculating limits of agreement, with small changes within a radius of <10% ignored due to the impact of measurement noise. Acceptable angular limits of agreement are ±30°, based on those proposed for cardiac output monitoring [25].

SV estimation agreement of the pulse contour model is presented in Refs. [11,26], and is not assessed here as it is not the focus of this study.

2.8. Frank-Starling curves

For each pig and intervention a Frank-Starling plot using measured and estimated *LEDV* & *SV* is created. A 7-beat median filter of measured and estimated *LEDV* & *SV* is calculated to mitigate the impact of abnormal heart beats, and measurement noise. For each intervention with a sufficient response (i.e. not a non-responsive intervention), a pig-specific linear-least-squares line of best fit for the *LEDV-SV* relationship is identified. R^2 is a measure of goodness of fit to a linear model. An acceptable R^2 is defined as $R^2 \geq 0.65$, so 65% of the variation in *SV* is explained by the linear model. This criterion acknowledges some variation in *SV* will result from temporal or disease driven changes such as from changing afterload, cardiac contractility, systemic resistance and/or arrhythmia [13,20], while largely adhering to the linear model. Overall, this choice is a lower limit measure of good correlation between these variables [27]. Additional higher limits of $R^2 \geq 0.75$ and $R^2 \geq 0.85$ are also considered, where $R^2 \geq 0.85$ represents strong correlation in this context. Bland-Altman analysis is used to assess the agreement of model-estimated *FSC* with measured *FSC* using [23].

3. Results

3.1. Response to interventions

Table 1 shows d_{95}, used to identify non-responsive interventions. Of 38 interventions across all pigs, 8 of 12 total fluid infusions and 1 RM were non-responsive interventions. Fig. 4 shows the ROC curve for identifying non-responsive interventions using $d_{95,est}$. A cut-off for $d_{c,est}$ between 0.274 and 0.279 maximised *TPR* − *FPR*. Balanced accuracy for this cut-off value was 0.82.

A summary table of measured signals during each intervention for each pig is given in appendix Table A.1.

3.2. LEDV estimation

Fig. 5 shows each pig's $\overline{LEDV}_{mea}$ and $\overline{LEDV}_{est}$ responses to each intervention type. Additionally, *LEDV* errors are given in appendix Table A.2. Fig. 6 shows Bland-Altman analysis of $\overline{LEDV}_{est}$ agreement with $\overline{LEDV}_{mea}$, and polar plot analysis of $\overline{LEDV}_{est}$ trending ability. Bland-Altman median bias and limits of agreement [2.5th, 97.5th percentile] of 2 ml [-14, 23] are well within the criterion of ±35 ml. Polar plot analysis angular limit of agreement is ±33°, slightly poorer than the target limit of ±30°.

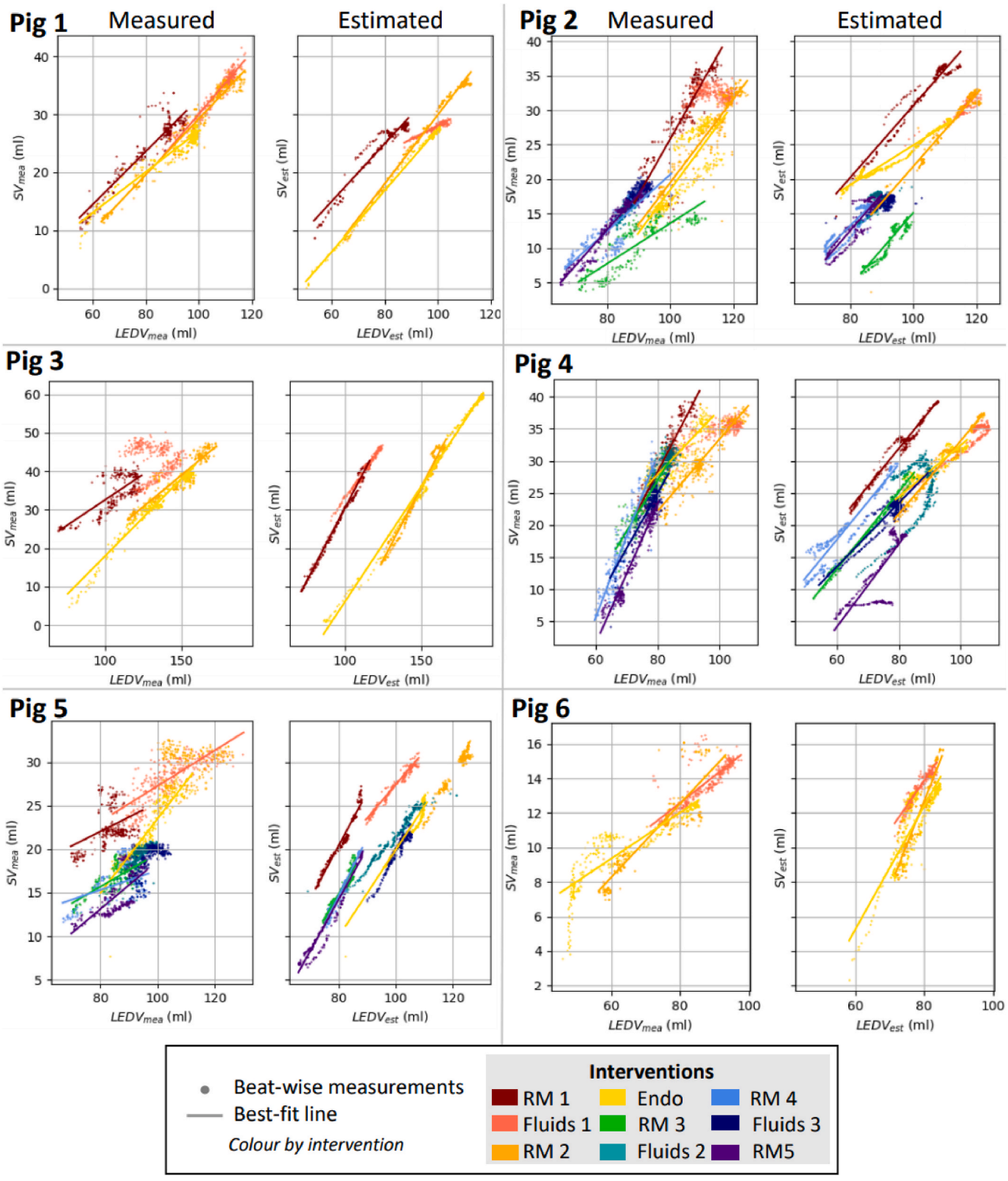

Fig. 7. Frank-Starling curves and line of best fit from measured and estimated values for each intervention for each pig. For clarity, 300 beats from each intervention are plotted as points, but all beats are used in line of best fit calculation.

3.3. Frank-Starling curves

Fig. 7 shows the Frank-Starling curves and line of best fit used to find *FSC*. R^2 values and *FSC* from each line of best fit, both measured and estimated, are given in Table 2. Using $LEDV_{mea}$ and SV_{mea}, a linear model was acceptable ($R^2_{mea} \geq 0.65$) for 24 of 29 responsive interventions. Also, 17 of 29 interventions had $R^2_{mea} \geq 0.75$, and 13 of 29 interventions had a strong correlation ($R^2_{mea} \geq 0.85$). Fig. 8 shows the Bland-Altman agreement of FSC_{est}, with FSC_{mea}. Median bias and limits of agreement are

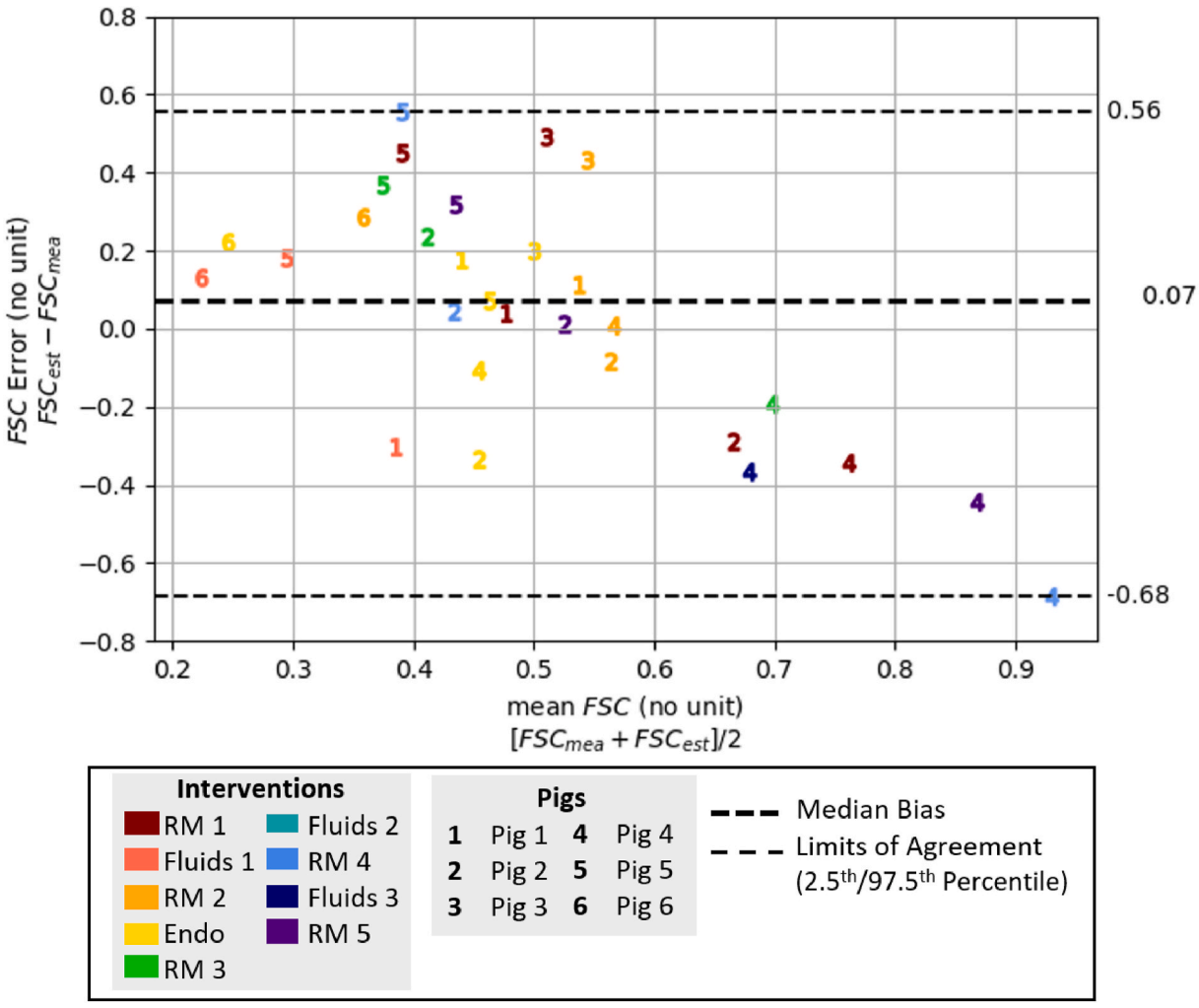

Fig. 8. Bland-Altman plot showing agreement of measured and estimated *FSC*. Errors for each responsive intervention are shown.

0.07 [-0.68, 0.56] for *FSC* from each pig and intervention.

4. Discussion

4.1. Response to interventions

Using $LEDV_{est}$ and SV_{est} to calculate $d_{95,est}$ and establish non-responsive interventions yielded a good ROC curve AUC of 0.83 (Fig. 4) and reasonable balanced accuracy of 0.82. Thus, model-based, non-additionally invasive $LEDV_{est}$ and SV_{est} are potentially good metrics to clinically assess whether a patient responds to treatment. Note, this definition of non-responsive is where *LEDV* and *SV* changes are small relative to measurement precision, and thus patient state is in a small cluster on the Frank-Starling curve.

The optimal $d_{c,est}$ established from the ROC curve of 0.276 is slightly higher than the defined $d_{c,mea}$ of 0.200, reflecting the increased uncertainty from model-estimated $LEDV_{est}$ & SV_{est}. This optimal value may also reflect smaller numbers in the ROC curve of Fig. 4. This $d_{c,est}$ yielded 9 FP and 1 FN. Pig 5 in particular had 4 FP interventions, marginal cases for which $d_{95,mea}$ and $d_{95,est}$ were both near to their respective cut-off values. The optimisation criterion using $TPR - FPR$ equally weights sensitivity and specificity. In the specific context of assessing fluid-responsiveness to determine whether fluids should be administered, it is important to avoid incorrectly identifying patients as responsive, which could lead to unnecessary fluid delivery and potentially harmful fluid overload [9]. Thus, a differently weighted optimisation criterion could be preferable to avoid the incidence of false negatives.

4.2. LEDV estimation

RMs led to a reduction in preload, which tended to have a similar effect for a given pig, but differ between pigs (Fig. 5). Fluid infusions increased preload at first and later plateaued, and the extent to which preload increased varied between pigs (Fig. 5). A total of 8 of 12 fluid infusions were non-responsive interventions (Table 1), for which *SV/LEDV* changes during the intervention were small relative to *SV/LEDV* measurement precision, based on the $d_{95,mea} < 0.2$ criterion. Endotoxin infusion and ensuing shock reduced *LEDV* for all pigs, with different trajectories for each pig (Fig. 5). All responses and variability between pigs matched expectations.

$\overline{LEDV}_{est}$ had good agreement with $\overline{LEDV}_{mea}$ with median bias and limits of agreement of 2.2 ml [-13.8, 22.5] (Fig. 6A), well within the acceptance criterion of ±35 ml. Trending ability was reasonable with an angular limit of agreement of 33° (Fig. 6B), just outside the criterion of 30°. The low bias and good agreement of this non-additionally invasive, continuous *LEDV* monitoring method make it a promising potential clinical tool for hemodynamic monitoring.

4.3. Frank-Starling curves

The measured *LEDV-SV* relationship was linear for most interventions, with $R^2 \geq 0.65$ for 24 of 29 interventions (Table 2), and a

strong linear correlation ($R^2 \geq 0.85$) was measured for 13 of 29 interventions. This linear relationship meets expectations based on [28,29]. Thus, it is reasonable to characterise the Frank-Starling relationship using a linear model, using the gradient from the line of best fit, *FSC*.

FSC estimated from each intervention had low bias but wide limits of agreement of 0.07 [-0.68, 0.56] (Fig. 8). The limited number of interventions/pigs makes it challenging to reliably assess the accuracy and precision of *FSC* estimation.

FSC potentially provides a useful clinical metric to characterise cardiac muscle performance as it reflects the force-length relation, and thus contractility, of cardiac muscle [30]. While contractility lacks a precise definition [31], *FSC* provides a readily interpretable metric based on known physiological responses and is dynamically identified from cardiac performance during a perturbation. Also, *FSC* is potentially useful for predicting and controlling *SV* responses for a therapy that induces a known change in preload, a holy-grail of hemodynamic management [3]. Note, E_{es} from the *LEDV* model (Equation (2)) is also a measure of contractility, in this case identified from the phenomenological relationship between E_{es} and *HR* [10]. This is a sufficient assumption for delivering good *LEDV* estimates but in the context of monitoring contractility this identification of E_{es} offers no additional information beyond measuring *HR* changes. On the other hand, *FSC* is information rich, based on the response of multiple physiological variables to a perturbation.

4.4. Limitations

4.4.1. Experimental interventions

A controlled pig trial differs from critically ill patients. First, while the anatomy of the porcine and human cardiovascular systems is similar, there are differences [32]. Second, the pig trial enables higher fidelity pressure catheter signals, where clinically, pressure catheters have more potential for artefacts [33,34]. Third, interventions in this trial, while designed to mirror ICU treatments, will not be directly equivalent, and may not reflect the entire range of physiological states seen in the ICU. The effect of RMs is diminished as pigs have an open chest held closed with clamps. However, the controlled pig trial enables validation measurements of *SV* with an aortic flow probe and *LEDV* with an admittance catheter, and interventions not feasible in a clinical scenario, all of which are useful for validating this method.

This study includes a limited number of pigs and intervention types. Thus, relationships shown in this study may not necessarily hold true under different physiological conditions. In particular, it would be useful to trial an intervention aiming to induce changes in contractility, such using inotropes, to assess how *FSC* and other physiological variables respond. However, the interventions trialled did achieve a large range of physiological states, with large ranges of pressures and SVs during the interventions (Table A.1). Thus, these data provide a robust validation set, where the results presented justify further optimisation and validation with human data.

4.5. Model assumptions

The models used are simple, lumped parameter models, which do not account for spatially varying information. As a result they will not capture all complex phenomena contributing to pressure-volume relationships in the circulation. An *SV* model able to account for arterial wave reflection may be more appropriate clinically, but would require an additional, typically invasive, pulse wave velocity measurement as an input [35]. The models chosen require fewer inputs, while still delivering acceptable accuracy/precision [11].

Both *SV* and *LEDV* models rely on an input pressure, P_{mea}, as their primary input. Artefacts in this signal, or local phenomena causing arterial pressure changes at the pressure catheter site, will lead to error. However, arterial pressure signals are routinely used in the ICU, with a waveform potentially rich in information, making them a good input clinically.

The model requires calibration which may introduce error. First, sensor drift and/or shift in physiological factors affecting model assumptions and calibration parameter values, such as changes in vasoconstriction, blood volume and disease onset, may introduce error such that recalibration is required. Second, the need for calibration during a period of stable hemodynamics is important as rapid changes in P_{mea}, or arrhythmia, during calibration will affect waveform shape, and thus parameter estimates, creating poor calibration values. In this study, neither of these present a major concern, as over a 30 min period these factors are expected to change only a small amount. Finding a 10-beat period of stable P_{mea} was achieved for all interventions.

The methodology used in this study to generate Frank-Starling curves, and thus calculate $d_{95,est}$ and FSC_{est}, could be applied to other clinically applicable measures of *LEDV* and *SV*. Non-additionally invasive *SV* measures are reviewed in Ref. [36]. The authors are unaware of any other non-additionally invasive, continuous *LEDV* measures. Echocardiography provides non-invasive intermittent measurement of *LEDV* [24], and invasive thermodilution/PAC methods provide continuous *LEDV* monitoring [37].

4.6. Frank-Starling curves

The ability to establish the Frank-Starling relationship, and thus *FSC*, is ultimately limited by the accuracy and precision of *LEDV* and *SV* measurements. With more precise measures, smaller responses could reliably be detected, and the slope of the relationship could be better identified. The results shown here are limited to responses with $d_{95} \geq 0.2$, which is still clinically potentially useful.

The Frank-Starling relationship, originally conceived by Starling for an isolated heart-lung preparation [6], is the preload-*SV* relationship when other factors, namely afterload and inotropy, are constant. For the in-tact circulation, afterload and inotropy cannot be made constant independently of preload because these factors are inextricably linked. Studies investigating the Frank-Starling relationship *in vivo* observe a linear relationship for the *LEDV*-Stroke work (*SW*) relationship [28,38] and *LEDV-SV* relationship [39], findings which likely reflect autoregulatory mechanisms where arterial afterload is adapted in response to *LEDV* changes [40]. Adjusting for afterload changes in the calculation of the Frank-Starling curves could produce the 'true' preload-*SV* relationship, but would add to the complexity of the method. This study uses the observed *LEDV-SV* relation as a clinically identifiable and readily interpretable relationship, with a focus on *SV* rather than *SW* given the end-goal of hemodynamic management to ensure perfusion through the body.

4.7. Translational considerations

Clinical validation is needed given the preliminary nature of these results whose predominant outcome is demonstrating the potential of these non-invasive, model-based methods. Validation of *LEDV* and *SV* could be measured using echocardiography, or a pulmonary artery catheter (PAC) where clinically appropriate. A key challenge is if clinical interventions/disease processes induce changes sufficiently large in relation to echocardiography/PAC precision to identify Frank-Starling curves. This issue could potentially be mitigated with repeated interventions to reduce noise by averaging, such as via a passive leg raise repeated several times. Establishing an appropriate frequency of recalibration is an important translational consideration to address during clinical validation. Clinical monitoring is typically for a much longer duration (hours) than the interventions in these studies ($\leq$30 min), thus sensor and physiological factors may change over this time-frame requiring recalibration.

5. Conclusions

This study provides proof-of-concept preload changes and Frank-Starling curves could be non-additionally invasively estimated for critically ill patients. For a pig trial during hemodynamic interventions, the ability of model-based, non-additionally invasive *LEDV* and *SV* to identify non-responsive interventions was good, as shown by ROC analysis. Model-based *LEDV* showed good Bland-Altman agreement and polar plot trending performance, using an admittance catheter as a reference method. Model-based *LEDV* and *SV* estimation were used to produce Frank-Starling curves, and thus estimate *FSC*. Hence, these preliminary results show these metrics could potentially provide clinicians with more insight into the efficacy of treatment and physiological mechanisms contributing to circulatory failure at the patient bedside.

Declaration of competing interest

The authors declare that they have no conflicts of interest for the study titled "***Preload & Frank-Starling curves, from textbook to bedside: clinically applicable non-additionally invasive model-based estimation in pigs***" submitted to *Computers in Biology and Medicine*.

Acknowledgements

This work was supported with funding from the University of Canterbury Doctoral Scholarship, MedTech CoRE, Royal Society of New Zealand Engineering Technology-based Innovation in Medicine consortium grant, and EU FP7 International Research Staff Exchange Scheme. The funders had no role in study design, data collection and analysis, decision to publish or preparation of the manuscript.

A Additional results.

Table A.1
Summary of measured signals for each intervention for each pig. All values are presented as median and 95% range [2.5th percentile, 97.5th percentile]. N is the number of beats. $\overline{P}$ refers to beat-wise mean pressure. PP refers to pulse pressure.

	Intervention	N	SV_{mea}	$LEDV_{mea}$	$\overline{P_{mea}}$	P_{mea} PP	$\overline{P_{cv}}$	HR
			ml		mmHg			bpm
Pig 1	RM 1	493	26 [11,33]	87 [56, 96]	51 [30, 56]	37 [14, 42]	12.1 [11.4, 15.1]	62 [61, 64]
	Fluids 1	1748	34 [25, 41]	109 [91, 116]	60 [52, 61]	41 [36, 42]	12.7 [11.4, 13.5]	58 [57, 60]
	RM 2	459	30 [12,39]	100 [64, 118]	52 [31, 58]	35 [8,38]	13.4 [12.7, 16.3]	58 [57, 59]
	Endo	317	25 [11,30]	97 [57, 101]	53 [26, 55]	33 [3,35]	12.8 [12.3, 14.7]	57 [57, 58]
Pig 2	RM 1	506	31 [14,38]	106 [89, 116]	54 [42, 56]	37 [24,40]	5.3 [4.4, 6.9]	66 [62, 71]
	Fluids 1	1600	32 [29,35]	115 [105, 122]	55 [53, 56]	40 [38, 42]	9.1 [5.5, 10.1]	63 [49, 88]
	RM 2	493	28 [13,35]	115 [95, 125]	55 [43, 56]	38 [24, 41]	8.8 [8.3, 10.5]	62 [46, 93]
	Endo	1967	19 [13,29]	103 [92, 117]	49 [44, 54]	30 [24,38]	9.7 [9.0, 10.4]	66 [51, 79]
	RM 3	566	12 [4,16]	89 [71, 110]	42 [29, 45]	23 [13,27]	10.1 [9.5, 11.4]	72 [67, 75]
	Fluids 2	2172	16 [13,18]	86 [82, 90]	51 [48, 53]	37 [32,39]	10.3 [9.1, 11.0]	67 [61, 75]
	RM 4	534	14 [7,19]	84 [68, 94]	46 [34, 50]	34 [22,39]	10.0 [9.3, 10.8]	68 [60, 73]
	Fluids 3	2273	18 [15,20]	90 [84, 96]	46 [44, 48]	37 [33,40]	9.9 [8.4, 10.8]	65 [59, 73]
	RM 5	506	14 [5,18]	81 [66, 93]	42 [30, 45]	30 [17,34]	9.9 [9.2, 10.9]	64 [58, 69]
Pig 3	RM 1	615	35 [24, 43]	109 [71, 124]	44 [29, 52]	27 [10,36]	5.6 [5.1, 6.5]	77 [68, 90]
	Fluids 1	2176	44 [35, 49]	133 [108, 153]	53 [46, 54]	38 [28,40]	7.2 [5.6, 8.3]	73 [55, 101]
	RM 2	545	38 [28, 47]	152 [116, 175]	46 [35, 53]	29 [14,37]	6.4 [5.8, 7.5]	69 [53, 94]
	Endo	1566	32 [8, 41]	136 [85, 160]	48 [26, 55]	25 [1,36]	7.4 [5.8, 9.4]	70 [53, 96]
Pig 4	RM 1	789	31 [21, 41]	84 [74, 92]	77 [68, 84]	31 [27,35]	4.4 [3.7, 6.8]	101 [81, 129]
	Fluids 1	3114	35 [29,39]	102 [83, 108]	84 [77, 86]	36 [31,38]	5.5 [4.0, 6.5]	87 [79, 109]
	RM 2	734	30 [20,38]	93 [81, 108]	84 [72, 89]	32 [27,37]	5.7 [5.1, 8.8]	91 [88, 96]
	Endo	2754	29 [24,39]	81 [75, 97]	78 [72, 89]	29 [25,36]	6.8 [4.8, 7.6]	88 [82, 93]
	RM 3	648	25 [11,31]	77 [67, 83]	53 [41, 63]	25 [19,27]	6.4 [5.8, 8.2]	82 [72, 90]
	Fluids 2	2988	30 [24,34]	83 [77, 88]	64 [54, 67]	32 [25,34]	6.0 [5.0, 6.8]	83 [68, 94]
	RM 4	680	17 [4,33]	69 [61, 79]	37 [29, 57]	22 [16,33]	7.0 [5.8, 8.6]	85 [80, 91]
	Fluids 3	2866	23 [10,29]	78 [67, 82]	46 [34, 49]	31 [20,32]	9.6 [7.0, 11.1]	82 [78, 87]
	RM 5	574	15 [5,25]	73 [62, 80]	34 [24, 42]	22 [12,28]	10.6 [10.2, 11.9]	75 [52, 84]
Pig 5	RM 1	582	22 [18,28]	83 [70, 94]	42 [34, 46]	31 [23,39]	5.9 [4.6, 6.6]	74 [65, 83]
	Fluids 1	1896	29 [23,33]	102 [88, 131]	45 [41, 47]	35 [31,37]	12.1 [8.0, 15.3]	68 [55, 85]
	RM 2	944	30 [25,33]	107 [98, 134]	46 [40, 48]	35 [29,37]	14.5 [12.2, 15.6]	66 [55, 84]
	Endo	1979	20 [17,28]	95 [84, 116]	39 [37, 43]	26 [22,33]	11.3 [9.4, 12.3]	66 [58, 79]
	RM 3	505	17 [13,19]	86 [70, 95]	35 [31,38]	19 [14,23]	6.5 [6.0, 7.1]	64 [55, 74]
	Fluids 2	2176	19 [16,21]	94 [84, 101]	35 [33,38]	22 [18,26]	8.6 [6.3, 11.7]	60 [51, 72]
	RM 4	463	16 [12,20]	88 [68, 98]	35 [31,38]	21 [17,26]	13.2 [11.6, 14.1]	58 [51, 68]
	Fluids 3	1776	19 [15,21]	97 [88, 107]	39 [33,40]	25 [19,26]	15.7 [13.4, 17.3]	59 [50, 71]
	RM 5	482	14 [11,19]	86 [70, 96]	32 [27,38]	15 [10,21]	15.3 [14.3, 16.8]	61 [51, 71]
Pig 6	Fluids 1	1851	14 [11,16]	86 [72, 97]	44 [41, 46]	38 [33, 41]	3.4 [2.6, 5.2]	73 [71, 75]
	RM 2	560	11 [6,16]	73 [54, 91]	38 [31, 42]	23 [13,31]	6.8 [4.7, 8.8]	70 [68, 71]
	Endo	1600	10 [5,13]	59 [47, 87]	39 [32, 43]	29 [13,32]	8.1 [6.9, 10.0]	72 [69, 75]

Table A.2
LEDV estimation error for each pig and intervention. Error is calculated in ml using $LEDV_{est} - LEDV_{mea}$, then converted to a percentage. All values are presented as median [2.5th, 97.5th percentile] of all beats from that intervention.

	Intervention	$LEDV_{mea}$	$LEDV_{est}$	*LEDV* Error	
		ml	ml	ml	%
Pig 1	RM 1	87 [56, 96]	82 [56, 89]	−1 [-14, 8]	−1 [-18, 11]
	Fluids 1	109 [91, 116]	101 [90, 104]	−7 [-13, −0]	−7 [-12, −0]
	RM 2	100 [64, 118]	104 [66, 112]	2 [-17, 16]	2 [-18, 20]
	Endo	97 [58, 101]	99 [54, 101]	1 [-4, 9]	1 [-7, 10]
Pig 2	RM 1	106 [89, 117]	107 [83, 115]	−0 [-18, 9]	−0 [-17, 8]
	Fluids 1	115 [105, 122]	117 [111, 120]	3 [-5, 9]	2 [-4, 9]
	RM 2	115 [95, 125]	118 [96, 121]	3 [-9, 10]	2 [-7, 9]
	Endo	103 [92, 117]	98 [78, 112]	−9 [-17, 5]	−9 [-17, 5]
	RM 3	89 [71, 110]	94 [84, 99]	5 [-16, 16]	6 [-15, 23]
	Fluids 2	86 [82, 90]	88 [83, 91]	2 [-2, 6]	3 [-3, 8]
	RM 4	84 [68, 94]	82 [72, 88]	−2 [-13, 9]	−2 [-15, 12]
	Fluids 3	90 [84, 96]	92 [86, 95]	1 [-4, 6]	2 [-4, 7]
	RM 5	80 [66, 93]	84 [72, 90]	2 [-8, 11]	3 [-9, 16]
Pig 3	RM 1	109 [71, 124]	103 [73, 117]	−5 [-30, 27]	−4 [-27, 32]
	Fluids 1	134 [108, 153]	116 [96, 124]	−24 [-38, 10]	−18 [-25, 9]
	RM 2	152 [116, 175]	150 [126, 166]	0 [-19, 24]	0 [-12, 18]
	Endo	136 [85, 160]	158 [90, 190]	25 [1,39]	18 [1,28]
Pig 4	RM 1	84 [74, 92]	81 [64, 92]	−3 [-11, 2]	−3 [-14, 2]
	Fluids 1	102 [83, 108]	105 [83, 109]	3 [-3, 9]	3 [-3, 9]
	RM 2	93 [81, 108]	97 [80, 107]	2 [-3, 7]	2 [-3, 8]
	Endo	81 [75, 97]	83 [79, 102]	3 [-4, 8]	3 [-4, 10]
	RM 3	77 [67, 83]	73 [55, 84]	−4 [-14, 4]	−5 [-20, 5]
	Fluids 2	83 [77, 88]	88 [71, 92]	4 [-7, 8]	5 [-9, 10]
	RM 4	69 [61, 79]	60 [50, 78]	−8 [-13, 1]	−12 [-20, 2]
	Fluids 3	78 [67, 82]	78 [59, 81]	−1 [-9, 3]	−1 [-13, 5]
	RM 5	73 [62, 80]	76 [60, 82]	2 [-4, 8]	2 [-6, 12]
Pig 5	RM 1	83 [70, 94]	82 [73, 88]	−1 [-12, 8]	−2 [-13, 11]
	Fluids 1	102 [88, 131]	103 [91, 108]	−1 [-24, 8]	−1 [-18, 9]
	RM 2	107 [98, 134]	123 [111, 126]	11 [-9, 25]	11 [-7, 25]
	Endo	95 [84, 116]	103 [97, 111]	9 [-6, 14]	10 [-5, 17]
	RM 3	86 [70, 95]	82 [75, 86]	−3 [-13, 5]	−3 [-14, 7]
	Fluids 2	94 [84, 101]	102 [86, 111]	7 [-6, 19]	8 [-6, 21]
	RM 4	88 [68, 98]	81 [76, 88]	−3 [-18, 9]	−4 [-19, 13]
	Fluids 3	97 [88, 107]	102 [92, 106]	5 [-7, 12]	5 [-6, 14]
	RM 5	86 [70, 96]	76 [66, 88]	−10 [-18, 3]	−11 [-22, 3]
Pig 6	Fluids 1	86 [72, 97]	79 [73, 84]	−8 [-14, 2]	−9 [-15, 3]
	RM 2	73 [54, 91]	78 [70, 85]	8 [-8, 19]	11 [-10, 33]
	Endo	59 [47, 87]	77 [64, 86]	17 [-2, 26]	30 [-3, 53]

References

[1] L. Busse, D.L. Davison, C. Junker, L.S. Chawla, Hemodynamic monitoring in the critical care environment, Adv. Chron. Kidney Dis. 20 (2013) 21–29.
[2] J.C. Orban, Y. Walrave, N. Mongardon, B. Allaouchiche, L. Argaud, F. Aubrun, G. Barjon, J.-M. Constantin, G. Dhonneur, J. Durand-Gasselin, H. Dupont, M. Genestal, C. Goguey, P. Goutorbe, B. Guidet, H. Hyvernat, S. Jaber, J.-Y. Lefrant, Y. Mallédant, J. Morel, A. Ouattara, N. Pichon, A.-M. Guérin Robardey, M. Sirodot, A. Theissen, S. Wiramus, L. Zieleskiewicz, M. Leone, C. Ichai, AzuRea, causes and characteristics of death in intensive care units, Anesthesiology 126 (2017) 882–889.
[3] T. Desaive, O. Horikawa, J.P. Ortiz, J.G. Chase, Model-based management of cardiovascular failure: where medicine and control systems converge, Annu. Rev. Contr. 48 (2019) 383–391.
[4] M.R. Pinsky, D. Payen, Functional hemodynamic monitoring, Crit. Care 9 (2005) 566.
[5] R.E. Peverill, Understanding preload and preload reserve within the conceptual framework of a limited range of possible left ventricular end-diastolic volumes, Adv. Physiol. Educ. 44 (2020) 414–422.
[6] Starling, The linacre lecture on the law of the heart given at cambridge, 1915, Nature 101 (1918), 43–43.
[7] F. Michard, S. Alaya, V. Zarka, M. Bahloul, C. Richard, J.-L. Teboul, Global end-diastolic volume as an indicator of cardiac preload in patients with septic shock *, Chest 124 (2003) 1900–1908.
[8] T.M. Enomoto, L. Harder, Dynamic indices of preload, Crit. Care Clin. 26 (2010) 307–321.
[9] P.E. Marik, Hemodynamic parameters to guide fluid therapy, Transfus. Altern. Transfus. Med. 11 (2010) 102–112.
[10] S. Davidson, C. Pretty, A. Pironet, S. Kamoi, J. Balmer, T. Desaive, J.G. Chase, Minimally invasive, patient specific, beat-by-beat estimation of left ventricular time varying elastance, Biomed. Eng. Online 16 (2017).
[11] J. Balmer, C.G. Pretty, S. Davidson, T. Mehta-Wilson, T. Desaive, R. Smith, G. M. Shaw, J.G. Chase, Clinically applicable model-based method, for physiologically accurate flow waveform and stroke volume estimation, Comput. Methods Progr. Biomed. 185 (2020) 105125.
[12] T. Luecke, P. Pelosi, Clinical review: positive end-expiratory pressure and cardiac output, Crit. Care 9 (2005) 607–621.
[13] M. Merx, C. Weber, Sepsis and the heart, Circulation 116 (2007) 793–802.
[14] J. Balmer, C. Pretty, S. Davidson, T. Desaive, S. Kamoi, A. Pironet, P. Morimont, N. Janssen, B. Lambermont, G.M. Shaw, J.G. Chase, Pre-ejection period, the reason why the electrocardiogram Q-wave is an unreliable indicator of pulse wave initialization, Physiol. Meas. 39 (2018), 095005.
[15] X.X. Yang, L.A. Critchley, D.K. Rowlands, Z. Fang, L. Huang, Systematic error of cardiac output measured by bolus thermodilution with a pulmonary artery catheter compared with that measured by an aortic flow probe in a pig model, J. Cardiothorac. Vasc. Anesth. 27 (2013) 1133–1139.
[16] S. Kutty, A.T. Kottam, A. Padiyath, K.R. Bidasee, L. Li, S. Gao, J. Wu, J. Lof, D. A. Danford, T. Kuehne, et al., Validation of admittance computed left ventricular volumes against real-time three-dimensional echocardiography in the porcine heart, Exp. Physiol. 98 (2013) 1092–1101.
[17] K. Sagawa, The end-systolic pressure-volume relation of the ventricle: definition, modifications and clinical use, Circulation 63 (1981) 1223–1227.
[18] J. Baan, E.T.V.D. Velde, Sensitivity of left ventricular end-systolic pressure-volume relation to type of loading intervention in dogs, Circ. Res. 62 (1988) 1247–1258.
[19] J. Balmer, R. Smith, C.G. Pretty, T. Desaive, G.M. Shaw, J.G. Chase, Accurate end systole detection in dicrotic notch-less arterial pressure waveforms, J. Clin. Monit. Comput. 35 (2020) 79–88.
[20] J.E. Hall, A.C. Guyton, Guyton and Hall Textbook of Medical Physiology, Elsevier, 2016.
[21] N. Westerhof, J.-W. Lankhaar, B.E. Westerhof, The arterial Windkessel, Med. Biol. Eng. Comput. 47 (2009) 131–141.
[22] K.H. Zou, A.J. O'Malley, L. Mauri, Receiver-operating characteristic analysis for evaluating diagnostic tests and predictive models, Circulation 115 (2007) 654–657.

[23] D.G. Altman, J.M. Bland, Measurement in medicine: the analysis of method comparison studies, The Statistician 32 (1983) 307.
[24] S. Malm, S. Frigstad, E. Sagberg, H. Larsson, T. Skjaerpe, Accurate and reproducible measurement of left ventricular volume and ejection fraction by contrast echocardiography, J. Am. Coll. Cardiol. 44 (2004) 1030–1035.
[25] L.A. Critchley, X.X. Yang, A. Lee, Assessment of trending ability of cardiac output monitors by polar plot methodology, J. Cardiothorac. Vasc. Anesth. 25 (2011) 536–546.
[26] R. Smith, J. Balmer, C.G. Pretty, T. Mehta-Wilson, T. Desaive, G.M. Shaw, J. G. Chase, Incorporating pulse wave velocity into model-based pulse contour analysis method for estimation of cardiac stroke volume, Comput. Methods Progr. Biomed. 195 (2020) 105553.
[27] H. Motulsky, Intuitive Biostatistics, Oxford University Press, 1995.
[28] D.D. Glower, J.A. Spratt, N.D. Snow, J.S. Kabas, J.W. Davis, C.O. Olsen, G.S. Tyson, D.C. Sabiston, J.S. Rankin, Linearity of the frank-starling relationship in the intact heart: the concept of preload recruitable stroke work, Circulation 71 (1985) 994–1009.
[29] U.F. Wiersema, S. Bihari, The frank-starling curve is not equivalent to the fluid responsiveness curve, Crit. Care Med. 45 (2017) e335–e336.
[30] R. Jacob, B. Dierberger, G. Kissling, Functional significance of the frank-starling mechanism under physiological and pathophysiological conditions, Eur. Heart J. 13 (1992) 7–14.
[31] W.W. Muir, R.L. Hamlin, Myocardial contractility: historical and contemporary considerations, Front. Physiol. 11 (2020) 222.
[32] P.P. Lelovas, N.G. Kostomitsopoulos, T.T. Xanthos, A comparative anatomic and physiologic overview of the porcine heart, J. Am. Assoc. Lab. Anim. Sci. 53 (2014) 432–438.
[33] R.M. Gardner, Direct blood pressure measurement —dynamic response requirements, Anesthesiology 54 (1981) 227–236.
[34] S. Romagnoli, Z. Ricci, D. Quattrone, L. Tofani, O. Tujjar, G. Villa, S.M. Romano, A. R.D. Gaudio, Accuracy of invasive arterial pressure monitoring in cardiovascular patients: an observational study, Crit. Care 18 (2014) 644.
[35] R. Smith, L. Murphy, C.G. Pretty, T. Desaive, G.M. Shaw, J.G. Chase, Tube-load model: a clinically applicable pulse contour analysis method for estimation of cardiac stroke volume, Comput. Methods Progr. Biomed. 204 (2021) 106062.
[36] B. Saugel, M. Cecconi, J. Wagner, D. Reuter, Noninvasive continuous cardiac output monitoring in perioperative and intensive care medicine, Br. J. Anaesth. 114 (2015) 562–575.
[37] C. Hofer, L. Furrer, S. Matter-Ensner, M. Maloigne, R. Klaghofer, M. Genoni, A. Zollinger, Volumetric preload measurement by thermodilution: a comparison with transoesophageal echocardiography, Br. J. Anaesth. 94 (2005) 748–755.
[38] S. Silvestry, The in vivo quantification of myocardial performance in rabbits: a model for evaluation of cardiac gene therapy, J. Mol. Cell. Cardiol. 28 (1996) 815–823.
[39] J.V. Nixon, R.G. Murray, P.D. Leonard, J.H. Mitchell, C.G. Blomqvist, Effect of large variations in preload on left ventricular performance characteristics in normal subjects, Circulation 65 (1982) 698–703.
[40] H. Takaoka, H. Suga, Y. Goto, K. Hata, M. Takeuchi, Cardiodynamic conditions for the linearity of preload recruitable stroke work, Heart Ves. 10 (1995) 57–68.